

## **SANDIA REPORT**

SAND2004-5277

Unlimited Release

Printed November, 2004

# **Nanoporous-Carbon Adsorbers for Chemical Microsensors**

M. P. Siegal, D. L. Overmyer, W. G. Yelton, A. W. Staton, P. P. Provencio,

Prepared by  
Sandia National Laboratories  
Albuquerque, New Mexico 87185 and Livermore, California 94550

Sandia is a multiprogram laboratory operated by Sandia Corporation,  
a Lockheed Martin Company, for the United States Department of Energy's  
National Nuclear Security Administration under Contract DE-AC04-94AL85000.

Approved for public release; further dissemination unlimited.



Issued by Sandia National Laboratories, operated for the United States Department of Energy by Sandia Corporation.

**NOTICE:** This report was prepared as an account of work sponsored by an agency of the United States Government. Neither the United States Government, nor any agency thereof, nor any of their employees, nor any of their contractors, subcontractors, or their employees, make any warranty, express or implied, or assume any legal liability or responsibility for the accuracy, completeness, or usefulness of any information, apparatus, product, or process disclosed, or represent that its use would not infringe privately owned rights. Reference herein to any specific commercial product, process, or service by trade name, trademark, manufacturer, or otherwise, does not necessarily constitute or imply its endorsement, recommendation, or favoring by the United States Government, any agency thereof, or any of their contractors or subcontractors. The views and opinions expressed herein do not necessarily state or reflect those of the United States Government, any agency thereof, or any of their contractors.

Printed in the United States of America. This report has been reproduced directly from the best available copy.

Available to DOE and DOE contractors from

U.S. Department of Energy  
Office of Scientific and Technical Information  
P.O. Box 62  
Oak Ridge, TN 37831

Telephone: (865)576-8401  
Facsimile: (865)576-5728  
E-Mail: [reports@adonis.osti.gov](mailto:reports@adonis.osti.gov)  
Online ordering: <http://www.osti.gov/bridge>

Available to the public from

U.S. Department of Commerce  
National Technical Information Service  
5285 Port Royal Rd  
Springfield, VA 22161

Telephone: (800)553-6847  
Facsimile: (703)605-6900  
E-Mail: [orders@ntis.fedworld.gov](mailto:orders@ntis.fedworld.gov)  
Online order: <http://www.ntis.gov/help/ordermethods.asp?loc=7-4-0#online>



## **Nanoporous-Carbon Adsorbers for Chemical Microsensors**

M. P. Siegal and D. L. Overmyer  
Advanced Materials Sciences Department

W. G. Yelton  
Photonic Microsystems Technologies Department

A. W. Staton  
Micro-Total-Analytical Systems Department

P. P. Provencio  
Radiation-Solid Interactions Department

Sandia National Laboratories  
P.O. Box 5800  
Albuquerque, NM 87185-1421

### **ABSTRACT**

Chemical microsensors rely on partitioning of airborne chemicals into films to collect and measure trace quantities of hazardous vapors. Polymer sensor coatings used today are typically slow to respond and difficult to apply reproducibly. The objective of this project was to produce a durable sensor coating material based on graphitic nanoporous-carbon (NPC), a new material first studied at Sandia, for collection and detection of volatile organic compounds (VOC), toxic industrial chemicals (TIC), chemical warfare agents (CWA) and nuclear processing precursors (NPP). Preliminary studies using NPC films on exploratory surface-acoustic-wave (SAW) devices and as a  $\mu$ ChemLab membrane preconcentrator suggested that NPC may outperform existing, irreproducible coatings for SAW sensor and  $\mu$ ChemLab preconcentrator applications. Success of this project will provide a strategic advantage to the development of a robust, manufacturable, highly-sensitive chemical microsensor for public health, industrial, and national security needs. We use pulsed-laser deposition to grow NPC films at room-temperature with negligible residual stress, and hence, can be deposited onto nearly any substrate material to any thickness. Controlled deposition yields reproducible NPC density, morphology, and porosity, without any discernable variation in surface chemistry. NPC coatings  $> 20 \mu\text{m}$  thick with density  $< 5\%$  that of graphite have been demonstrated. NPC can be "doped" with nearly any metal during growth to provide further enhancements in analyte detection and selectivity.

Optimized NPC-coated SAW devices were compared directly to commonly-used polymer-coated SAWs for sensitivity to a variety of VOC, TIC, CWA and NPP. In every analyte, NPC outperforms each polymer coating by multiple orders-of-magnitude in detection sensitivity, with improvements ranging from  $10^3$  to  $10^8$  times greater detection sensitivity! NPC-coated SAW sensors appear capable of detecting most analytes tested to concentrations below parts-per-billion. In addition, the graphitic nature of NPC enables thermal stability  $> 600 \text{ }^\circ\text{C}$ , several hundred degrees higher than the polymers. This superior thermal stability will enable higher-Temperature preconcentrator operation, as well as greatly prolonged device reliability, since polymers tend to degrade with time and repeated thermal cycling.

# Acknowledgements

The authors thank D. R. Tallant for Raman analysis. Supported by Laboratory Directed Research and Development, Sandia is a multiprogram laboratory operated by Sandia Corporation, a Lockheed Martin Company, or the United States Department of Energy's National Nuclear Security Administration under contract DE-AC04-94AL85000.

# Table of Contents

Abstract .....	iii
Acknowledgements .....	iv
I. Introduction .....	1
II. Nanoporous-carbon films for gas microsensors .....	3
III. Acoustic loss in SAW sensor coatings .....	13
IV. Comparing nanoporous-carbon to polymers .....	18
V. Summary .....	25
VI. Publications and Presentations .....	27
Distribution List .....	28

## Tables

2.1 NPC density and thickness for each SAW coating .....	5
3.1 NPC density and resulting SAW acoustic loss .....	14
3.2 NPC density and fitted parameters for acetone adsorption isotherms .....	15

## Figures

2.2 TEMs of NPC film with different density .....	6
2.3 SAW response vs. NPC density for 5% acetone .....	7
2.4 SAW response vs. acetone concentration vs. NPC density .....	7
2.5 SAW response for different analytes at 5% .....	8
2.6 Log-log SAW response vs. acetone concentration vs. NPC density .....	9
2.7 Prefactor and power-law vs. NPC density for acetone .....	10
2.8 Extrapolated SAW response for acetone vs. NPC density .....	11
3.1 SEMs of various nanotextured SAW coatings .....	13
3.2 SEMs of NPC films with different density .....	14
3.3 Log-log acetone SAW response vs. NPC density .....	15
3.4 Extrapolated SAW response for acetone vs. NPC density .....	16
3.5 SAW acoustic loss and power law vs. NPC density .....	17

4.1	SAW step function response to acetone and toluene vs. coating	18
4.2	SAW step function response to iso-octane, chlorobenzene, and TCE vs. coating	19
4.3	SAW step function response to DIMP vs. coating	20
4.4	SAW adsorption isotherms for acetone vs. coating	21
4.5	SAW adsorption isotherms for acetone following DIMP exposure vs. coating	22
4.6	SAW adsorption isotherms for toluene vs. coating	22
4.7	SAW adsorption isotherms for iso-octane vs. coating	23
4.8	SAW adsorption isotherms for chlorobenzene vs. coating	23
4.9	SAW adsorption isotherms for TCE vs. coating	24

# Nanoporous-Carbon Adsorbers for Chemical Microsensors

## I. INTRODUCTION

Sensor systems that rapidly detect airborne chemicals are critically important to public health, national security and nonproliferation. Volatile organic compounds (VOC), toxic industrial chemicals (TIC), chemical warfare agents (CWA) and nuclear processing precursors are four compound classes of interest. All are implicated in terrorist activities and constitute security threats to the country. Examples of these airborne chemicals are:

1. VOCs: acetone, alcohols, benzene, etc.
2. TICs: acrylonitrile, methyl vinyl ketone, toluene di-isocyanate, etc.
3. CWA simulants: dimethyl methylphosphonate (DMMP), chloroethyl isoamyl sulfide
4. nuclear processing precursors: tributyl phosphate

Robust sensors and micro-total analytical systems depend largely on coatings compatible with environmental factors such as temperature, humidity, and the chemical background. These coatings need to be manufacturable, sensitive, reproducible, and durable for long-term use. Two functions of coatings are of interest: (1) preconcentrator coatings that only release adsorbed material thermally and (2) sensor coatings sensitive to partial vapor pressures.

Chemical microsensors rely on partitioning of airborne compounds into chemically-selective films to collect and measure trace quantities of hazardous vapors. For the MicroChemLab, low-level contaminants are captured into an adsorbent sol-gel preconcentrator film for subsequent analysis. However, these sol-gel layers are constrained to submicron thicknesses due to high residual stresses, limiting the total surface area available for physio- or chemi-adsorption. This stress can lead to delamination of the film or cracking the preconcentrator thin membrane during thermal cycling. A slow aging process also exists that may make sol-gels ineffective for long-term monitoring applications. Hydrophobic sol gels, while at first effective, become more hydrophilic over time, presenting stability challenges to long-term field uses critical to chemical monitoring for national security. Identifying a stress-free porous media is necessary. In addition, given the ubiquitous presence of water in the environment, the main interferent to chemical sensing, hydrophobic materials, such as graphitic-type carbons, are preferred.

Sensor coatings for surface acoustic wave (SAW) devices are currently based on polymers deposited by spray- or spin-coating. Again, thickness limits exist due to dampening of the surface-acoustic wave. This dampening is a function of film thickness, poor film rigidity, and material density. Additionally, residual stresses lead to delamination and cracking. Coating reproducibility is an enormous problem due to several factors (manual operation, solution viscosity and rheology) that determine the final thickness and film morphology. Other

approaches tested have incompatible deposition steps, precluding their use of the same substrate. Self-assembly or electrochemical deposition are examples where concurrent deposition becomes problematic. Poorly applied polymer coatings often de-wet during use, leading to unpredictable and reduced chemical responses. Polymers also lack the sensitivity and speed of response necessary for low-level (ppb) detection of VOCs and TICs.

This project studied nanoporous-carbon (NPC) for SAW sensor coatings. All data collected in this work are directly transferable to preconcentrator coatings used in the Sandia MicroChemLab. Advantages of using SAW detectors for this study include the ability to test a variety of analytes in a wide range of concentrations with ease. SAW sensors can also be used to perform chemical adsorption experiments on NPC coatings, critical information for using NPC as a sensor coating. We grow NPC using pulsed-laser deposition (PLD) at room-temperature with negligible residual stress. Therefore, NPC coats nearly any substrate material, including microfabricated membranes, to any thickness. We have already grown > 20- $\mu\text{m}$  thick NPC films. NPC density, and hence, porosity, is precisely controlled, allowing the total graphitic carbon surface area to be tailored for a particular device or application. Density can range from 2.0 – 0.08  $\text{g}/\text{cm}^3$  (pyrolytic graphite = 2.27  $\text{g}/\text{cm}^3$ ). No discernible variations in carbon chemistry are detected by Raman spectroscopy as a function of NPC density. Yet surface reactivity can be independently controlled via post-annealing without changing the NPC porous network structure.



## II. NANOPOROUS-CARBON FILMS FOR GAS MICROSENSORS

### INTRODUCTION

Gas-phase sensor systems that rapidly detect airborne chemicals are critical to public health and national security needs.<sup>1</sup> Volatile organic compounds (VOC), toxic industrial chemicals (TIC), and chemical warfare agents (CWA) are compound classes of interest. Examples are: (VOC) ketones, alcohols, aliphatics and aromatics; (TIC) chlorinated hydrocarbons and aromatics; and (CWA) nerve and mustard gases.

Robust sensors and micro-analytical systems depend on coatings compatible with environmental factors such as temperature, humidity and chemical background. These coatings need to be manufacturable, sensitive, reproducible, and stable for long-term use. Two functions of sensor coatings are of general interest: sensor coatings responsive to partial vapor pressures, and preconcentrator coatings that only release adsorbed analyte thermally.

Both surface acoustic wave (SAW) sensors and quartz crystal microbalances (QCM) measure the mass of materials that stick to the device surface. SAWs differ from bulk QCMs by using higher frequency oscillations that are sensitive only to mass changes in the surface region, resulting in greater analyte sensitivity and faster response times.<sup>2</sup> Sorbent sensor coatings for either SAW or QCM devices typically use sol-gels or polymers deposited by spray- or spin-coating.<sup>3,4</sup> Small shifts in the device vibrational frequency relate to the sorption of gas species. However, thickness constraints exist for these coatings due to dampening of the surface acoustic wave, limiting the total porous volume available for physi- or chemi-sorption. This dampening is a function of film thickness, film rigidity, and material density. Coating irreproducibility occurs due to factors such as manual operation, and solution viscosity and rheology that determine final film thickness and morphology. Alternate approaches, such as self-assembly and electrochemical deposition, require thin seed coatings that are often difficult to apply to the SAW substrate, precluding their use. Additionally, poorly applied polymer coatings can de-wet during use, leading to unpredictable and reduced chemical responses.<sup>5,6</sup> As a result of these limitations, polymer coatings lack the sensitivity, reproducibility, and stability necessary for parts-per-billion (ppb) detection of VOCs and TICs.

Porous sol-gel silica coatings and highly porous alumina coatings nearly free of acoustic dampening have also been reported for use as SAW microsensor coatings.<sup>7,8</sup> In all cases, the ultimate analyte sensitivity is limited by the sorbent layer thickness due to residual film stresses and acoustic losses.<sup>9</sup> Particularly important is that the thickness, and hence, sorbing surface area in these porous films is confined to macro and mesoporous structures, leading to device sorption limitations. In addition, sol-gel coatings demonstrate aging effects with time.

Preconcentrator devices consist of a highly sorbent coating, typically porous sol-gel silica, on a thin membrane with a microheater fabricated on the backside. Rapid heating in a few ms to ~ 200 °C thermally releases the captured analyte into some analytical system. However,

high-residual stresses in these coatings lead to film delamination and membrane cracking with thermal cycling, constraining films to submicron thicknesses that limit the available adsorbent surface area. Identifying a stress-free porous media is necessary. In addition, given the ubiquitous presence of water in the environment, the main interferent to chemical sensing, hydrophobic materials, such as graphitic-type carbons, are preferred.<sup>10,11,12,13,14,15</sup>

Recently, we reported the use of nanoporous-carbon (NPC) as a preconcentrator adsorbent for CWAs.<sup>16</sup> NPC is a purely graphitic form of carbon with highly controlled densities ranging from less than 0.1 to 2.0 g/cm<sup>3</sup>. With room-temperature growth and negligible residual stress, NPC coats nearly any substrate to any desired thickness. Deposition control yields precise density, thickness, morphology, and porosity. In this paper, we report on the microstructure of NPC as a function of mass density and its correlation with its properties as a VOC and TIC sensor coating for SAW devices.

## EXPERIMENT

**NPC Growth.** We grow NPC films using pulsed-laser deposition (PLD) as described elsewhere. Briefly, focused 248 nm excimer pulsed-laser radiation (KrF) ablates a rotating pyrolytic graphite target with energy density just above the carbon ablation limit,  $\sim 1 \text{ J/cm}^2$ . With base pressure  $< 10^{-7}$  Torr, we introduce a controlled pressure of Ar into the PLD chamber during growth to further attenuate the kinetic energy of the ablated species. As  $p(\text{Ar})$  increases, the kinetic energy of the ablated species decreases, resulting in lower NPC mass densities. The coatings for the SAW devices in this study were grown simultaneously with test films grown on Si substrates that were used for the structural measurements reported in ref. 16. Therefore, the thicknesses, densities and surface morphologies are identical to those presented in that paper.

**Substrates.** NPC films were grown onto three different substrates for this study. We deposited two thin films (a few nm's) with densities near 1.0 and 0.25 g/cm<sup>3</sup> onto "holey-carbon" grids for subsequent structural analysis by high-resolution transmission electron microscopy (TEM). No further sample preparation was required to perform TEM study. We also grew six NPC films with densities ranging from 0.18 – 1.08 g/cm<sup>3</sup> directly onto the surfaces of 97-MHz ST-quartz SAW delay lines described elsewhere. To reduce the issue of frequency dampening, all films were grown to a constant areal density  $\sim 0.138 \pm 0.005 \text{ mg/cm}^2$ , equivalent to  $\sim 0.6 \text{ }\mu\text{m}$  of high-density graphite (2.27 g/cm<sup>3</sup>). NPC films were grown simultaneously onto Si(100) substrates for physical property measurements. The actual density and thickness of each NPC coating used on the SAW devices are listed in Table 1.

**SAW Measurements.** We tested the adsorption properties of the NPC-coated SAW devices in a controlled acetone (a typical VOC) atmosphere with saturation pressures ranging from  $P/P_{\text{sat}} = 0.01 - 0.50$ . As analyte adsorbs into NPC, the oscillator frequency shifts downward. The SAW sensor measurement system is described elsewhere. Briefly, all six SAW devices, each with a different NPC density coating, operate simultaneously in the same ambient. Oscillator frequency measures to  $\pm 1 \text{ Hz}$  ( $\sim 10^{-2}$  ppm). The SAW devices mount into a brass fixture with

active temperature control to reduce frequency fluctuations. The fixture design provides excellent radio frequency shielding for the SAW devices. The detection of acetone by the devices is correlated with NPC density, providing information both to optimize NPC as a sensor material, as well as to understand the surface chemistry of NPC with respect to acetone. Other analyte gases at  $P/P_{\text{sat}} = 0.05$  also were tested for each NPC-density SAW device to determine the overall effectiveness of NPC as a general sensor material. These include other VOCs (cyclohexane, n-propanol, methanol, ethanol, benzene, and toluene) and some TICs (chlorobenzene, carbon tetrachloride, iso-octane, and trichloroethylene).

Density [ $\text{g}/\text{cm}^3$ ]	Thickness [ $\mu\text{m}$ ]
0.18	7.75
0.24	5.89
0.36	3.86
0.73	1.93
0.96	1.38
1.08	1.22

**Table 1:** Mass density and thickness of the NPC films coating each of the six SAW sensor devices. The mass areal density is maintained to be constant at  $0.138 \pm 0.005 \text{ mg}/\text{cm}^2$ .

## RESULTS

**NPC Structures via TEM.** Figures 2.1(a) and (b) show high-resolution TEM images for ultrathin layers of NPC deposited directly onto TEM grids with densities  $0.25$  and  $1.0 \text{ g}/\text{cm}^3$ , respectively. These images provide some insight into the ability of NPC to have such widely varying densities. First is the presence of voids in the material. These are difficult to capture with TEM for NPC due to both its highly disordered structure and the low atomic weight of carbon. Nevertheless, an arrow points to such a void near the center of fig. 2.1(a). Its shape is somewhat elliptical, with dimensions  $\sim 10 \times 14 \text{ \AA}$ . Interestingly, this is about the size of a fullerene molecule. We do not imply that fullerene molecules exist in NPC, but rather, that the alignment of curved graphene fragments are unlikely to enclose a void region smaller than such structures. Larger void structures are also likely to exist. A high-density of such voids create surface area for analyte adsorption.

The second feature of note is the interplanar spacings between graphene sheet fragments. There are regions in each image where several graphene sheet fragments line up sufficiently to allow measurement of the average interplanar spacing. A line is drawn through an example of such lined-up sheet fragments in each image. Several occurrences of these fragments exist in every image taken. For the  $0.25 \text{ g}/\text{cm}^3$  density sample in fig. 2.1(a), the spacing is  $5.2 \pm 0.2 \text{ \AA}$ . For the  $1.0 \text{ g}/\text{cm}^3$  density sample in fig. 2.1(b), the spacing is  $4.6 \pm 0.2 \text{ \AA}$ . Note that the interplanar spacing of high-density pyrolytic graphite =  $3.35 \text{ \AA}$ . Clearly as NPC density decreases, the interplanar graphene sheet fragment spacing increases. Intercalation of elements

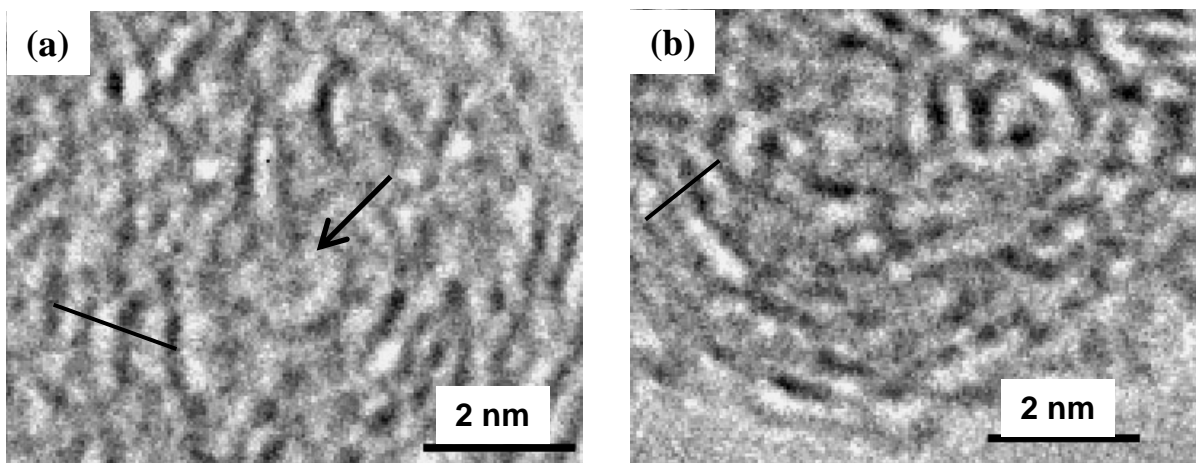


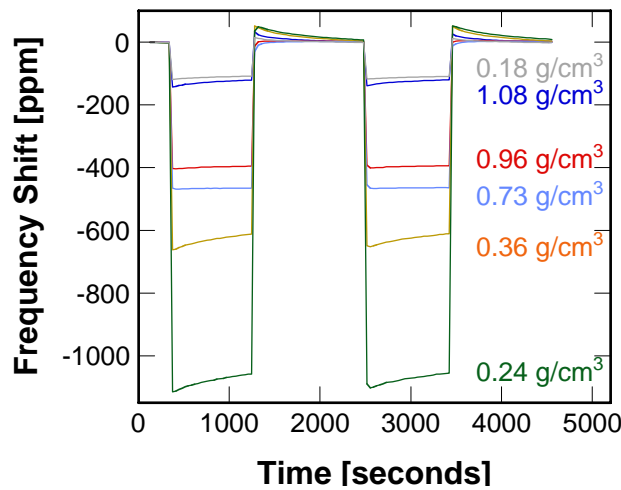
**Figure 2.1:** High-resolution TEM images of NPC films with densities: (a) 0.25 and (b) 1.0  $\text{g}/\text{cm}^3$ . An arrow points to a typical nanopore in (a). The straight lines are drawn as guides-to-the-eye for examples of the interplanar spacings between graphene sheet fragments.

and molecules into graphite is well known. Increasing the spacing between graphene sheets should ease diffusion both in and out of the coating.

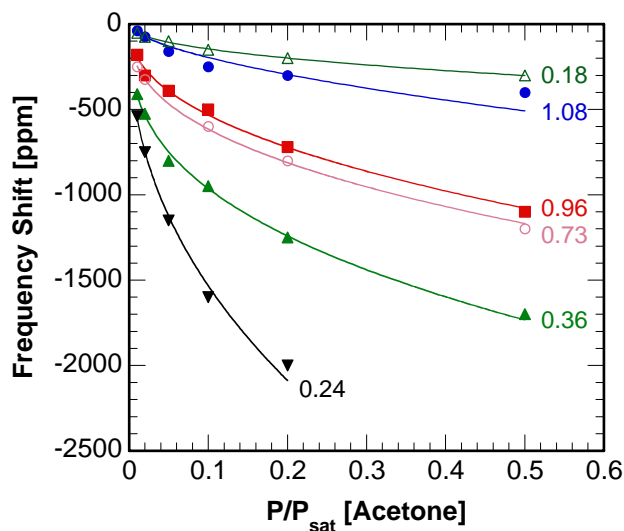
**Adsorption Isotherms for Acetone as a Function of NPC Density.** Fig. 2.2 shows the signal response from our SAW sensor measurement system for all six devices tested simultaneously in  $P/P_{\text{sat}}(\text{acetone}) = 0.05$ . Each device registers the presence of acetone exposure and then its removal as a function of time. Note the fast adsorption equilibrium and desorption times of just a few seconds for these NPC-coated devices. Cavitand-coated QCM sensors take tens of seconds for adsorption equilibrium and many minutes to achieve full desorption for detection of acetone.<sup>17</sup> Phospholipid, calixarene, cyclodextrin, and allyl-alcohol coated SAW sensors show a similar slow responses to VOCs.<sup>18,19,20,21</sup> From 1.08 to 0.24  $\text{g}/\text{cm}^3$ , the downward oscillator frequency shift responding to acetone increases with decreasing NPC density. Since the carbon areal density is constant in these coatings, lower density implies greater porosity and interplanar spacing, and hence, greater surface area. Only the lowest NPC density coating measured, 0.18  $\text{g}/\text{cm}^3$ , does not follow this trend. This is discussed below. It is worth noting that the sensitive response reported for carboxylate-coordinated  $\text{Cu}^{2+}$ -terminated surface coatings for the same acetone exposure is  $\sim 10$  ppm, which is about an order of magnitude lower than the worst response shown in fig. 2.2.<sup>22</sup>

Fig. 2.3 shows a direct correlation between NPC mass density and SAW sensor response to acetone for  $P/P_{\text{sat}}$  ranging from 0.01 to 0.50. The oscillator frequency responses fit a power law function for all SAWs and increase with decreasing NPC density. As noted above, only the lowest density NPC coating does not follow this trend, perhaps due to the weakness of such a fragile nanostructure limiting the transmission of an acoustic wave. Repetition of this coating always results in lesser sensitivities. NPC with density = 0.24  $\text{g}/\text{cm}^3$  provides the best response to acetone in the range of partial pressures studied. Indeed, the frequency shift for this device at

$P/P_{\text{sat}} = 0.50$  could not be made since it exceeded the capability of our measurement system. We also note that the response of this SAW device is 540 ppm at the lowest exposure,  $P/P_{\text{sat}} = 0.01$ . For comparison, fast-response polymer coatings such as PIB (polyisobutylene), PECH (polyepichlorohydrin) and FPOL (fluoropolol) were calibrated to have a linear frequency response in a range with maximum  $P/P_{\text{sat}} = 0.076$ , just below the minimum acetone concentration used in our experiment. In addition, these measurements were enhanced with the use of a preconcentrator. Nevertheless, extrapolating their results to  $P/P_{\text{sat}} = 0.01$  finds responses which measured only 1, 4, and 8 ppm, respectively, much lower than the 540 ppm measured for NPC.<sup>23</sup> Such large frequency responses of the NPC films obviously will result in greater signal-to-noise ratios and improve the reliability of SAW measurements for analytes in low concentrations.



**Figure 2.2:** Oscillator frequency response SAW devices taken simultaneously for six different NPC-coating densities with repetitive exposure to acetone at 5% saturation pressure.



**Figure 2.3:** SAW frequency response to controlled acetone exposures ranging from 1 – 50% saturation pressure for all six densities of NPC-coated devices.

**NPC-Coated SAW Results for VOCs and TICs.** Figure 2.4 shows the 0.24 g/cm<sup>3</sup> NPC coated-SAW response to exposure to a variety of gases at  $P/P_{\text{sat}}(\text{analyte}) = 0.05$ . Large shifts in oscillator frequency exist for each analyte tested. In particular, chlorinated hydrocarbons, ketones, and aromatics demonstrate strong adsorption into NPC. Other VOCs like alcohols have the weakest response at ~ 200 ppm. However this relatively weak response for alcohols is still significantly stronger than that for methanol with polymer-coated SAW devices which range from 0.4 – 5 ppm.<sup>24</sup> Note that dendrimer polymer coated 98 MHz SAW devices demonstrate shifts of 5, 4, and 8 ppm for exposures to  $P/P_{\text{sat}}(\text{analyte}) = 0.25$  for carbon tetrachloride, benzene, and trichloroethylene, respectively.<sup>25</sup> This compares with responses of 1070, 698, and 622 ppm, respectively, for NPC-coated SAW devices at exposures a factor of 5 less than those used in the dendrimer study. Siloxane-coated SAW devices report frequency responses for  $P/P_{\text{sat}}(\text{analyte}) = 0.05$  of toluene, methanol, acetone, and trichloroethylene of only 12, 12, 3, and 4 ppm, respectively. This compares to NPC-coated SAW device responses of 819, 197, 1081, and 622 ppm for the same analytes. Furthermore, for most of these examples in the literature, the SAW device response times to analytes are significantly longer, especially for recovery, than shown in fig. 2.2 for acetone, which is typical for all the analytes reported here.

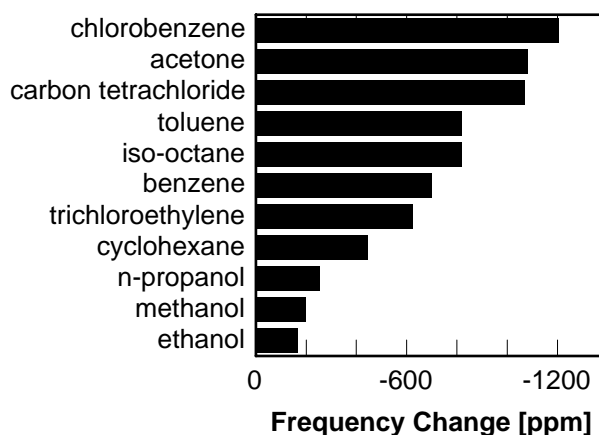


**Figure 2.4:** Bar graph showing the frequency response of the 0.24 g/cm<sup>3</sup> NPC-coated SAW device to various analytes at 5% saturation pressure.

## Discussion

Frequency shifts recorded for SAW devices relate to changes in mass density, temperature, and modulus of elasticity of the ST-cut quartz, coating conductivity, and coating stress. The latter four factors are negligible since: (a) the measurements are performed in a temperature-controlled environment; (b) no changes occur to the elasticity of the quartz; (c) NPC is a poor conductor due to its high-degree of disorder; and (d) NPC has no measurable stress. Only mass loading of analyte into the NPC coating perturbs the SAW propagation velocity, according to the following equation:

$$\Delta v = -\eta v_0^2 \Delta \rho \quad (1)$$

where  $\Delta\nu$  is the change in frequency due to the adsorption of the analyte into the NPC coating,  $\eta$  is the mass sensitivity factor of the ST-cut quartz substrate ( $1.3 \times 10^{-6} \text{ cm}^2/\text{g}$ ),  $\nu_0$  is the baseline frequency of the SAW oscillator ( $\sim 97 \text{ MHz}$ ), and  $\Delta\rho$  is the change in surface mass density due to the adsorption of the analyte into the NPC coating. Hence the y-axis of fig. 3 can be converted into areal mass density of acetone collected in the NPC-coated SAW device.

Furthermore, since the acetone isotherms shown in fig. 3 are power-law functions, they can be written in the form:

$$\Delta\rho = a \cdot (P/P_{\text{sat}})^m$$

where  $a$  is some prefactor and  $m$  is the power law. A linear relationship results from plotting in log-log form using the equation:

$$\log(\Delta\rho) = \log(a) + m \cdot \log(P/P_{\text{sat}}) \quad (3)$$

Figure 2.5 shows these linear relationships. The only exception to this linear behavior is the adsorbate isotherm for the highest density NPC coating tested, which exhibits saturation for  $P/P_{\text{sat}}(\text{acetone}) > 0.10$ . This may result from diffusion limitations due to low porosity, i.e. acetone adsorption occurring only in a fraction of the coating below the surface. Again, the adsorption data for the lowest density coating appears abnormally low. A possible reason for this may be a failure of structural integrity of the coating due to its nanostructure that must contain the largest pores, the thinnest pore wall structures, and the greatest interplanar spacings. These features would make such a structure highly susceptible to localized stress-induced damage from analyte adsorption onto its surfaces. Since either damage or stress changes the dependence of the SAW device oscillator frequency response, interpretation of this isotherm is convoluted and, hence, not included in the following discussions.

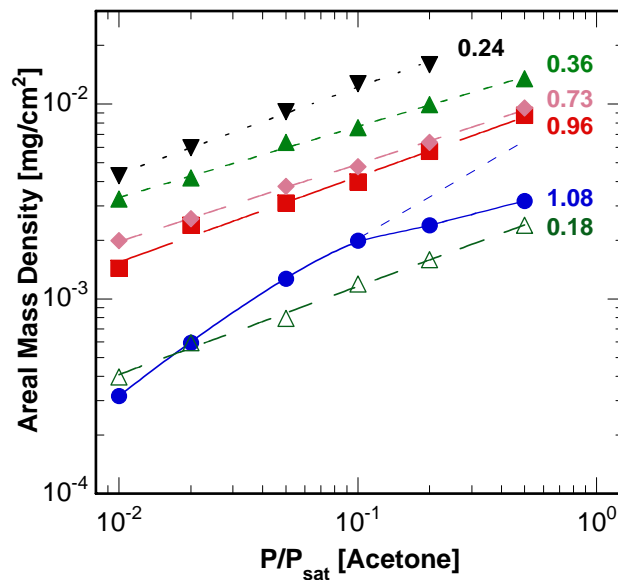


**Figure 2.5:** Log-log representation of total acetone adsorbed into NPC coatings as a function of acetone partial pressure for each NPC mass density studied.

Observation of figure 2.5 provides insight to the meaning of the prefactor,  $a$ , and the power law,  $m$ , as functions of NPC density. The prefactor, shown in fig. 2.6(a), represents the maximum mass loading the NPC-coating can adsorb in a fully saturated analyte stream. Clearly this relates to the available NPC surface area and we find that it increases with decreasing NPC density. Note that the SAW device coated with  $0.24 \text{ g/cm}^3$  density NPC to an areal density of  $0.13 \text{ mg/cm}^2$  can adsorb  $0.034 \text{ mg/cm}^2$  of acetone in a saturated stream, i.e. this NPC coating can adsorb 26 % of its mass in acetone. The data for the  $1.08 \text{ g/cm}^3$  coating is extrapolated to higher pressures from the results below its apparent saturation level; the resulting prefactor is consistent with those from the lower density NPC coatings. To first order, it appears advantageous to utilize NPC with the greatest possible surface area, i.e. the lowest density that maintains structural integrity.

The power law, shown in fig. 2.6(b), is the slope of the data curves in fig. 2.5. The flatter this slope, or the smaller the power law, the greater the response of the SAW device in low analyte concentrations. Physical interpretation of the power law, or response factor, will require further study. It may involve diffusion and sticking energies. Note that the response factor begins to increase for NPC density  $< 0.35 \text{ g/cm}^3$ , somewhat higher than the fall-off in the prefactor shown in fig. 6(a). Since saturation levels and response factors optimize for different NPC densities, it is likely that the chemical reactivity of NPC internal surfaces varies somewhat as a function of density.

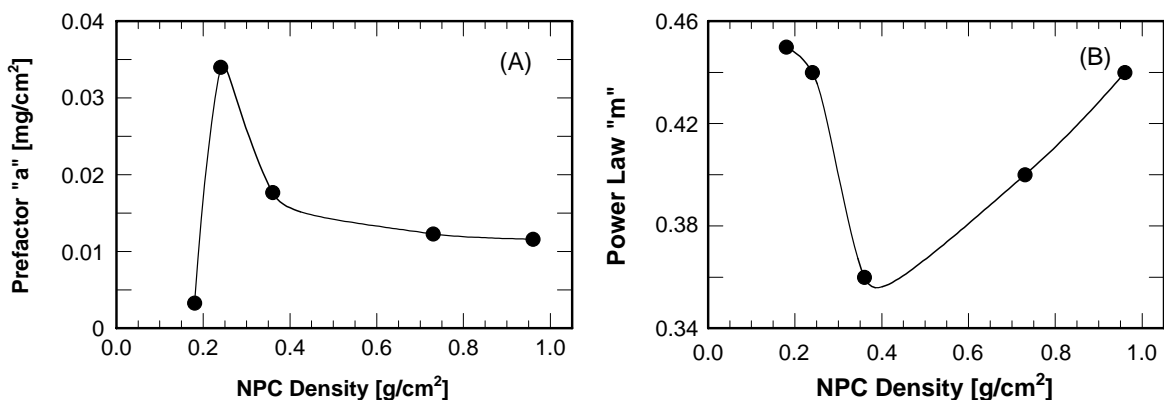


**Figure 2.6:** (a) The prefactor 'a', or the maximum acetone loading into a SAW coating and (b) the power law 'm', or the response factor, as functions of NPC density.

Using the above formulation of oscillator frequency response behavior allows prediction of the lowest possible analyte concentration that may be detectable for a given NPC-coated SAW device. Our SAW measurement system can resolve changes in oscillator frequency  $\sim 1$  Hz. From equation (1), this is equivalent to detecting a mass areal density change  $10^{-7} \text{ mg/cm}^2$ . Using this as a baseline, we extrapolate the adsorption isotherm results in figure 2.7 to very low concentrations. Note that  $P/P_{\text{sat}} = 10^{-9}$  is ppb. This extrapolation to low pressures



suggests that SAW devices coated with the appropriate density of NPC can detect acetone in concentrations  $< 1$  ppb. Experiments are planned to test these predictions.

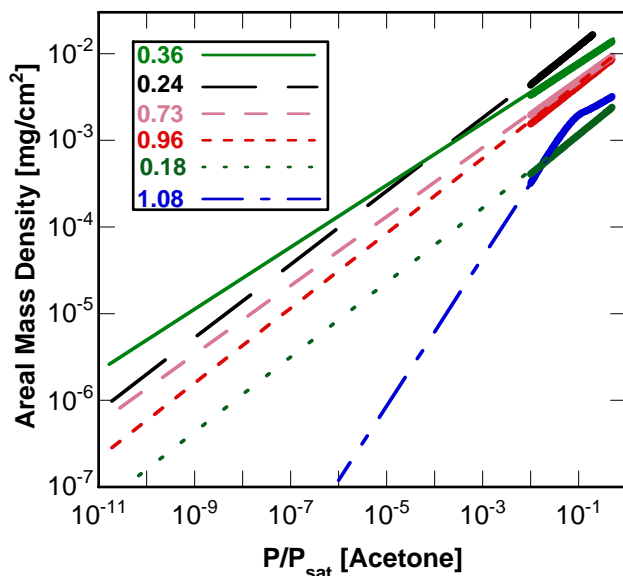


**Figure 2.7:** Extrapolation of the log-log graphical representation of the acetone adsorption isotherms to acetone concentrations below ppb.

## SUMMARY AND CONCLUSIONS

Nanoporous-carbon films grow at room-temperature with negligible residual stress, hence they can coat nearly any substrate to any thickness. Mass density is well-controlled by the deposition energetics and can be  $< 0.1 \text{ g/cm}^3$ . Decreasing density occurs by increasing nanopore size and density, and by increasing the spacing between graphene sheet fragments. These physical changes effectively increase available surface area for physi- or chemisorption of analyte gases. NPC-coated SAW devices readily detect a variety of VOCs and TICs with strong signals under modest exposures. We studied the acetone adsorption into NPC-coated SAWs in greater detail and find a power-law relationship between adsorption and analyte partial pressure. Analysis of this behavior suggests the possibility of detecting acetone below ppb concentrations using NPC with mass densities  $< 1.0 \text{ g/cm}^3$ . Ongoing research is further improving this sensitivity with further optimization of NPC-coating nanostructure, density and thickness.

## References:

---

- 1 Hughes, R. C.; Ricco, A. J.; Butler, M. A.; Martin, S. J. *Science* **1991**, 254, 74.
- 2 Murray, G. M.; Southard, G. E. *IEEE Instrumentation & Measurement Magazine* **2002**,  
Dec. 12.
- 3 Ricco, A. J.; Frye, G. C.; Martin, S. J. *Langmuir* **1989**, 5, 273.
- 4 Thomas, R. C.; Sun, L.; Crooks, R. M.; Ricco, A. J. *Langmuir* **1991**, 7, 620.
- 5 Grate, J. W.; McGill, R. A. *Anal. Chem.* **1995**, 67, 4015.
- 6 Stahl, U.; Rapp, M.; Wessa, T. *Analytica Chimica Acta* **2001**, 450, 27.
- 7 Hietela, S. L.; Smith, D. M.; Hietela, V. M.; Frye, G. C.; Martin, S. J. *Langmuir* **1993**, 9,  
249.
- 8 Yelton, W. G.; Pfeiffer, K. B.; Staton, A. W. *J. Electrochem. Soc.* **2002**, 149, H1
- 9 Lucklum, R.; Behling, C. Hauptmann, P. *Anal. Chem.* **1999**, 71, 2488.
- 10 Grate, J. W.; Abraham, M. H.; Du, C. M.; McGill, R. A.; Shuely, W. J. *Langmuir* **1995**,  
11, 2125.
- 11 Kruk, M.; Jaroniec, M.; Gadheree, K. P. *Langmuir* **1999**, 15, 1442.
- 12 Meszaros, R.; Nagy, M.; Varga, I.; Laszlo, K. *Langmuir* **1999**, 15, 1307.
- 13 Darkrim, F.; Levesque, D. *J. Phys. Chem.* **2000**, 104, 6773.
- 14 Nguyen, C.; Do, D. D. *Langmuir* **2001**, 17, 1552.
- 15 Lu, C.-J.; Zellers, E. T. *Anal. Chem.* **2001**, 73, 3449.
- 16 Siegal, M. P.; Overmyer, D. L.; Kottenstette, R. J.; Tallant, D. R.; Yelton, W. G. *Appl.*  
*Phys. Lett.* **2002**, 80, 3940
- 17 Hartmann, J.; Hauptmann, P.; Levi, S.; Dalcanale, E. *Sensors and Actuators* **1996**, B35-  
36, 154.
- 18 Enguang, D.; Guanping, F.; Zhenhua, H.; Dafu, C. *IEEE Trans. on Ultrasonics,*  
*Ferroelect. and Freq. Control* **1997**, 44, 309.
- 19 Yang, X.; Shi, J.; Johnson, S.; Swanson, B. *Sensors and Actuators* **1997**, B45, 79.
- 20 Yang, X.; Shi, J.; Johnson, S.; Holesinger, T.; Swanson, B. *Sensors and Actuators* **1997**,  
B45, 87.
- 21 Avramov, I. D.; Kurosawa, S. Rapp, M. Krawczak, P. Radeva, E. I. *IEEE Trans. on*  
*Microwave Theory and Techn.* **2001**, 49, 827.
- 22 Thomas, R. C.; Yang, H. C.; DiRubio, C. R.; Ricco, A. J.; Crooks, R. M. *Langmuir* **1996**,  
12, 2239.
- 23 Park, J.; Groves, W. A.; Zellers, E. T. *Anal. Chem.* **1999**, 71, 3877.
- 24 Zellers, E. T.; Baternan, S. A.; Han, M.; Patrash, S. J. *Anal. Chem.* **1995**, 67, 1092.
- 25 Tokohisa, H.; Crooks, R. M.; Ricco, A. J.; Osbourn, G. C.; *Electrochem. Soc. Proc.* **1997**,  
97-19, 134.

### III. ACOUSTIC LOSS IN SAW SENSOR COATINGS

Many different high-surface area materials have been studied for potential use as a gas-absorber for surface acoustic wave (SAW) device sensors. From the discussion in Section II, we know that small changes in the oscillator frequency response of a SAW device are primarily related to a change in the surface mass. As such, a number of nanotextured films have been studied. These are shown in fig. 3.1

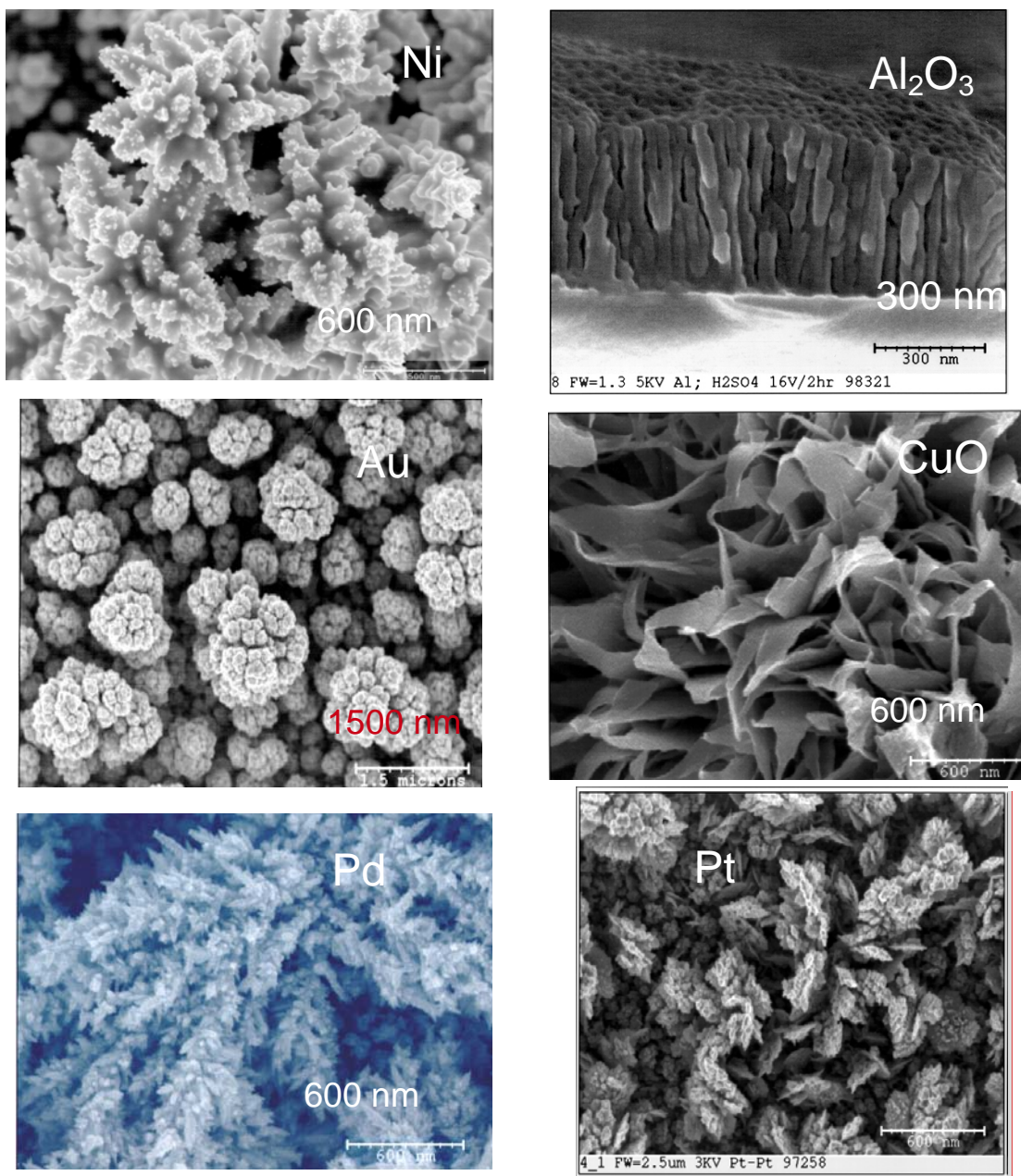


**Figure 3.1:** Nanotextured films of various metals and metal-oxides, with thicknesses ranging from 200 – 1500 nm, all grown electrochemically.

The material properties of these nanotextured film coatings on a SAW device contribute to acoustic dampening. Such acoustic dampening limits the usefulness of these otherwise high-surface area coatings for detection of analyte gases. As an example, a frequency scan of a bare SAW device yields a noise response typically near  $-10.5$  dB. However, the Pt film shown in fig. 3.1, which is only 200 nm thick, increases the noise level, or acoustic dampening, of such a device to  $-29$  dB. The CuO film has a noise level of  $-14.5$  dB. It is worth noting that these high acoustic noise responses are likely due to relatively high levels of residual stress within the coatings. Obviously, nanoporous-carbon (NPC), with its high surface area and negligible residual stress, has the possibility of better performance.

NPC mass density is controlled during growth by the  $p(\text{Ar})$  used to attenuate the kinetic energy of the ablated carbon species. Fig. 3.2 shows SEM images of the surfaces of two NPC films grown with different density, but with the same amount of total carbon mass. Table 3.1 shows the relationship between density and SAW sensor acoustic loss. Clearly, as mass density decreases, acoustic loss increases. However, this is different from the behavior observed in the nanostructured metals and metal-oxide coatings, since none of the NPC film coatings have any measurable residual film stress.

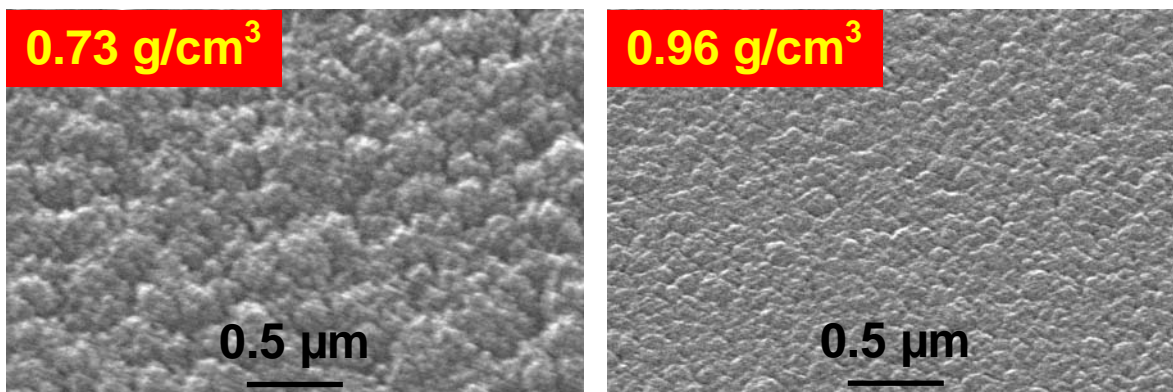


**Fig. 3.2:** SEM images showing the morphology of NPC films, each  $\sim 1$   $\text{mg}/\text{cm}^2$  in mass areal density.

NPC Density [ $\text{g}/\text{cm}^3$ ]	SAW Sensor Acoustic Loss
0.57	-28.46 dB
0.70	-19.25 dB
0.89	-12.33 dB
0.97	-11.82 dB

**Table 3.1:** The SAW sensor acoustic loss from NPC coatings of different mass density, however, with each having the same total mass areal density.

In section 2, we showed that NPC isotherms can be represented as power-law functions. Fig. 3.3 shows isothermal SAW adsorption data for acetone taken as a function of acetone partial pressure in the testing ambient for NPC films with different mass density. These coatings were

nominally  $1 \text{ mg/cm}^2$  thick, and to make the analysis more clear, the adsorption frequency shift data were normalized to this value. Clearly a range of acceptable NPC mass densities are found, from  $0.7 - 1.0 \text{ g/cm}^3$ . Only the SAW device with the lowest NPC density coating =  $0.57 \text{ g/cm}^3$  behaves differently. This low density film has greater signal response to high concentrations of acetone, however, appears to drop off much faster at lower concentrations of acetone analyte. These densities somewhat higher than those reported in the previous section due to improvements made in the optics of the pulsed-laser deposition (PLD) system over a period of time. These improvements enabled the growth of more homogeneous NPC films with greater sensitivity to low concentrations of analytes.

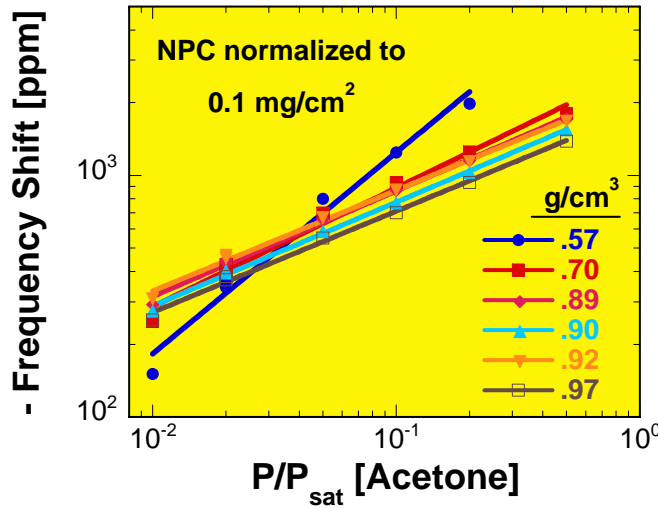


**Figure 3.3:** Log-log representation of total acetone adsorbed into NPC coatings as a function of acetone partial pressure for each NPC mass density studied.

Similar to the analysis shown in the last section, both a prefactor and slope of these curves yield information about total surface area and ability to collect data at low analyte concentrations. This is summarized in Table 3.2.

Density [ $\text{g/cm}^3$ ]	Prefactor “a”	Slope “m”
0.57	8480	0.83
0.70	2753	0.49
0.89	2350	0.44
0.90	2083	0.43
0.92	2267	0.42
0.97	1866	0.42

**Table 3.2:** NPC density and fitted parameters from data shown in fig. 3.3.

Using the fitted factors in Table 3.2, the data presented in fig. 3.3 can be extrapolated to low dilution concentrations of acetone. This is shown in fig. 3.4. Such extrapolation of the power-law isotherms suggests possible detection of acetone to concentrations well below 1 part-

per-billion (ppb). The vertical axis minimum is set to 0.1 ppm frequency shift of the SAW devices; this is more than ten times greater than the minimum detectable response. The x-axis, or acetone concentration, now has a minimum value of ppb. Obviously, the minimum predicted frequency shift should be capable of readily detecting ppb quantities of acetone.

Not shown, are measurements made using a diffusion tube experimental apparatus that allowed measurement of SAW devices at significantly lower concentrations. One such measurement was made for acetone, where the concentration of acetone was  $\sim 10$  ppm, or  $P/P_{sat} \sim 10^{-6}$ . The frequency shift of the device was  $\sim 50$  ppm. This fits directly on the extrapolated line in fig. 3.4!

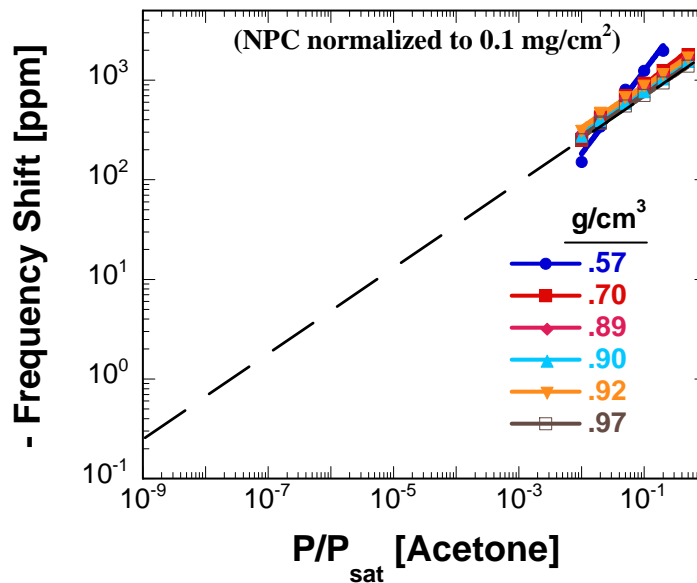


**Figure 3.4:** SAW isotherm data extrapolated to low acetone concentrations.

It is interesting to observe that a relationship appears to exist between the predicted performance of an NPC coating for a SAW device, the fitted slope from the isotherms, and the acoustic noise measured from the coated device. These two measurements are plotted together in fig. 3.5.

These studies demonstrate that acoustic loss in a SAW device is related to more than one coating parameter. The metal and metal-oxide coatings are examples of film stress causing noise in the response. As stress decreases, so does acoustic loss. This is the common problem experienced for SAW sensor coatings, which are typically polymer films, to be discussed in the next section. Indeed, polymer deposition is regulated by monitoring the acoustic loss during spray deposition. Once the loss reaches a certain value, the deposition ceases. These films are very thin compared to the NPC films studied here, due to significant residual stress associated with drying.

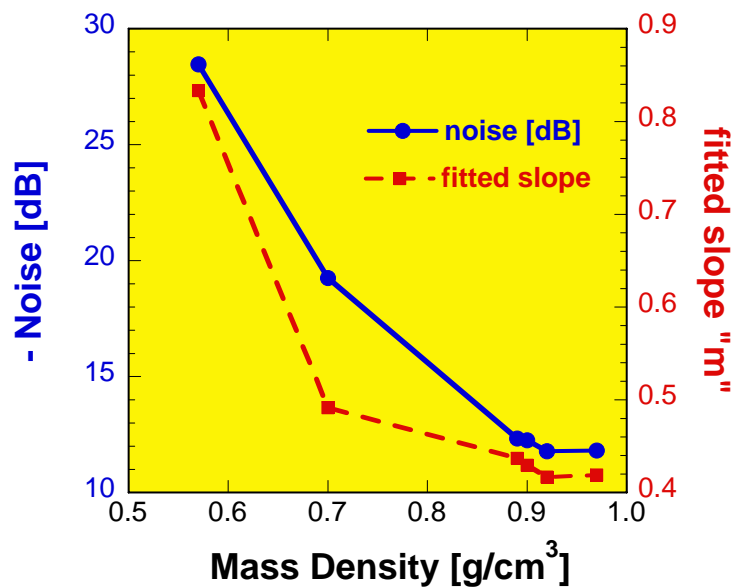


**Figure 3.5:** SAW acoustic loss and the fitted slope from acetone isotherm data vs. NPC mass density.

NPC has negligible residual stress. This means that the high acoustic loss measured for low-density NPC coatings has nothing to do with reaching a critical thickness due to the build-up of stress. Rather, the acoustic loss measured in NPC coated SAW devices is a measure of the ability of the coating to support an acoustic wave. Mechanically, this represents how well the clusters of deposited NPC are connected to one another. If the NPC film carbon clusters are too far apart, or connected with minimal graphene sheet fragments, then the acoustic loss will be high. When the carbon clusters are well-connected, they readily support transport of an acoustic wave and the loss is low.

A careful balance needs to be maintained to create an NPC with the ideal nanostructure for use in SAW devices. (1) A relatively low density, compared to graphite, must be used in order to have high surface area available for analyte adsorption. (2) The NPC material must be structurally sound so that it can support propagation of the acoustic wave. This sets a lower limit on the possible NPC mass density.

In summary, SAW sensors are sensitive to combinations of positive and negative influences that are coupled to the acoustic signal. Increasing stress and decreasing rigidity of a SAW coating can increase the initial acoustic loss of the sensor, limiting its usefulness at low analyte concentration exposures. Room-temperature growth of NPC by pulsed-laser deposition using a low-kinetic energy ablated carbon species can result in stress-free, high-surface area graphitic films with sufficient rigidity on any substrate to enable SAW sensor devices with remarkable analyte sensitivities.

#### IV. COMPARING NANOPOROUS-CARBON TO POLYMERS

Polymer films are most typically used as gas adsorbing coatings on SAW sensor devices. We directly compared the performance of nanoporous-carbon (NPC) with four different commonly used polymer materials:

PIB: poly(isobutylene)

PECH: poly(epichlororhydrin)

BSP-3: polymer developed by J. Grate from Pacific Northwest National Laboratory

DKAP: poly[2-(3-propylene)-3,5 bis(trifluoromethyl)phenol]methyl siloxane

Fig. 4.1 shows the step analyte exposures from two volatile organic compounds (VOCs), acetone and toluene, using each of these sensor materials on a SAW device. These exposures were made simultaneously in our analyte detection system described in Section III.

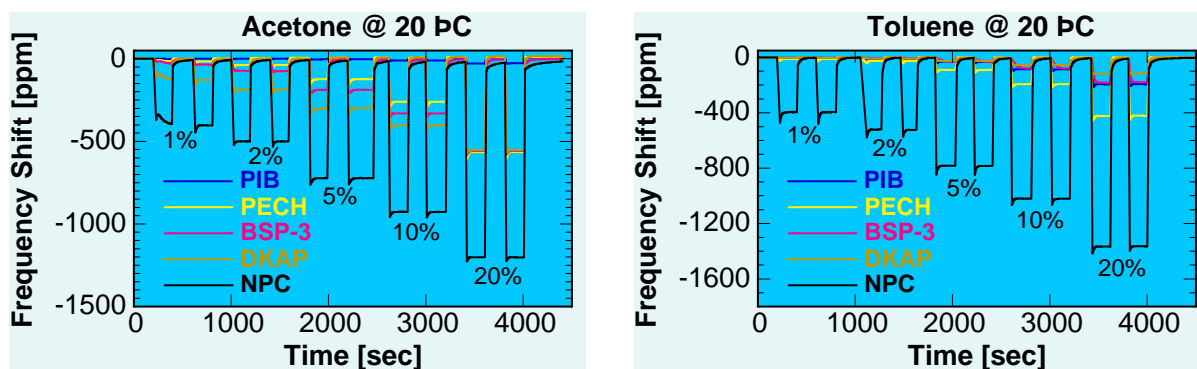


**Figure 4.1:** SAW frequency shift as a function of exposure to analyte (acetone or toluene). The percentages under each data set are the  $P/P_{\text{sat}}$ (analyte) used during that step exposure.

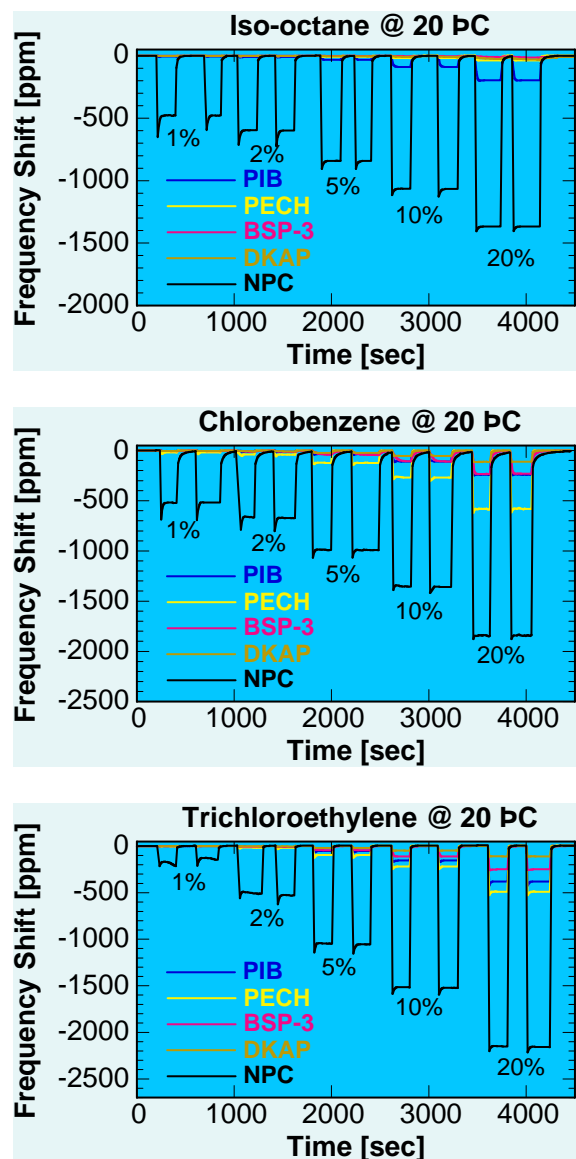
It is clear that NPC outperforms each polymer coating tested. It is worth noting that DKAP does a reasonably good job of detecting acetone, although the advantage demonstrated with NPC increases as the  $P/P_{\text{sat}}$  decreases, i.e. NPC appears to become an increasingly better sensor coating as partial pressure of analyte decreases to lower concentrations. And while PECH appears to outperform the other polymers in detecting toluene, none of the polymers appear particularly effective at the lowest concentrations measured, while NPC still registers very strong frequency shifts.

Fig. 4.2 shows the results from three different toxic industrial chemicals (TICs). The first is iso-octane, for which PIB is the only polymer that has a strong detection signal, but only at the highest concentrations studied. NPC again clearly outperforms all the polymers, and is the only absorbent with strong signals at 1%  $P/P_{\text{sat}}$ . The next two TICs studied were chlorinated compounds. Chlorobenzene is also extremely well-detected by NPC, with performance that



appears similar to iso-octane. The only competitive polymer is PIB, but again, only at the highest concentrations used.

Trichloroethylene (TCE) behaves noticeably different from the other analytes studied here. Again, NPC clearly outperforms all of the polymer films, however it is worth noting that even NPC shows a significant reduction in frequency shift at the lowest TCE concentration studied. The polymer coatings all have reasonable, although much weaker than NPC, responses at the highest concentrations used, with PECH leading the way. Nevertheless, the SAW sensor response using the polymer coatings all fall off dramatically at the lower TCE concentrations. In general, PECH does appear to be sensitive primarily to chlorinated TICs compared to the other coatings used in this comparative study. Such chemical discrimination is an excellent property for SAW sensor coating materials. Clearly, all results to date show that NPC is a uniformly good getter for nearly all gas-phase chemical compounds. A universal getter, such as NPC, is also an important sensor material. It is hoped that by doping or functionalizing NPC, such chemical selectivity can be built in later.



**Figure 4.2:** SAW frequency shift as a function of exposure to analyte (iso-octane, chlorobenzene, and TCE).

Finally, we also looked at the performance of these SAW sensor coatings for a semi-volatile chemical compound. Dimethyl (DIMP) is a nerve-gas simulant, i.e. a chemical warfare agent (CWA). We previously studied the use of NPC as a preconcentrator for dimethyl methylphosphonate (DMMP), another CWA nerve-gas simulant.<sup>1</sup> In that study it was found that NPC continued to adsorb, or preconcentrate, DMMP as a function of exposure time. The

coatings were flash heated to 200 °C in < 10 ms into a gas chromatograph. The absorption of DMMP into NPC was linear with time until the films were saturated. Their performance was as good as any of the standard used polymers at the time. What differentiates NPC from the polymers for use in a preconcentrator device is its intrinsically higher thermal stability. Raman spectroscopy suggests that NPC is stable to temperatures > 600 °C, while most of the polymers begin to decompose at temperatures ranging from 300 – 400 °C. The greater thermal stability of NPC will allow higher temperature operation for release of preconcentrated chemicals, providing two major advantages for NPC over polymers for use in a preconcentrator device. First, NPC will release certain semi-volatile chemicals that may not be able to be released from a polymer coating. This increases the range of chemicals that can be detected using a preconcentrator. Second, high-temperature flashing of even VOCs and TICs should provide sharper detection signals, i.e. greater precision and accuracy in both identifying the chemicals and determining their concentrations.

A SAW sensor device is an excellent tool to use to determine whether or not a given analyte can be preconcentrated into a particular coating. Figs. 4.1 and 4.2 show that all of the coatings used readily release each of the VOC and TIC analytes studied when the analyte is simply removed from the ambient. Fig. 4.3 shows similar data for DIMP. For this semi-volatile CWA, three of the coatings tested do not provide total release of DMMP at 20 °C: BSP-3, NPC, and DKAP. Each of these materials can be used as a preconcentrator for this CWA. However, both PIB and PECH act as typical SAW coatings, providing ready release of the analyte. It is worth noting that while PECH in particular has a reasonably strong SAW response at high concentrations of DIMP, it falls off dramatically at the lower concentrations where one would be more interested in detecting its presence.

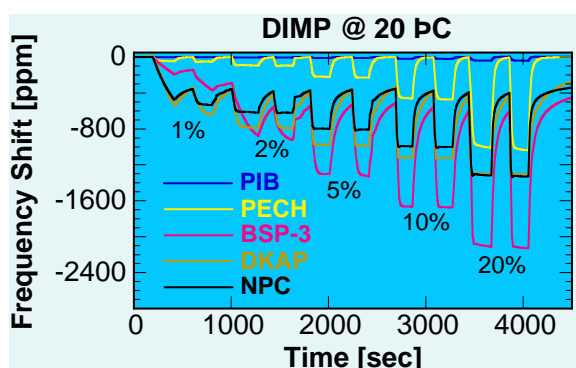


**Figure 4.3:** SAW frequency shift as a function of exposure to DIMP.

Note that while BSP-3 coated SAW devices show the strongest response at 20% saturation pressures, it falls off very quickly as the concentrations decreases. By  $P/P_{\text{sat}} = 1\%$ , DKAP and NPC are the most sensitive coatings. Furthermore, notice that upon release of DIMP from the ambient, both DKAP and NPC SAW devices show identical frequency responses independent of the actual exposure. This result indicates that DIMP is not only preconcentrated into these coatings to a fixed level, but that DIMP is now present in the coating until thermally released.

To a certain extent, one can consider DIMP to now be functionalizing both DKAP and NPC. Assuming that DIMP was a chemical that demonstrates chemical selectivity for adsorption onto its surface, then these results show that it is indeed possible to functionalize NPC, with its apparent enormous surface area, with a chemical that can provide selectivity. While we did not get the opportunity to address this issue in greater detail within the confines of this project, this result does point to the probability of success if the right functional chemicals are simply adsorbed into NPC. Finally, the advantage of NPC over DKAP or any polymer for such applications will be its significantly higher thermal stability.

In Section II, we showed that isotherm data for adsorption of acetone into NPC-coated SAW devices follow a power-law behavior. It turns out that all of the analytes studied follow power-laws, and not just for NPC, but for all of the polymer coatings studied as well. Furthermore, these data can be extrapolated to very dilute concentrations. This is shown in fig. 4.4 for SAW detection of acetone. The graph on the left shows that all of the data fit power-laws, with NPC demonstrating both the highest sensitivity (adsorption) over the range studied, and the lowest slope, or fall-off with decreasing acetone concentration, suggesting that NPC should out-perform each of the polymers at dilute acetone concentrations. The graph on the right extrapolates these data to ppb concentrations and device responses more than one order-of-magnitude above the detection limits. This extrapolation of the power-law suggests that NPC will be able to detect ppb concentrations of acetone with responses more than two orders-of-magnitude above the detection limits. Only DKAP offers even the remote possibility of ppb detection. The other polymer-coated SAW devices have acetone limits of detection (LOD) between 7 – 10 orders-of-magnitude below that inferred for NPC.

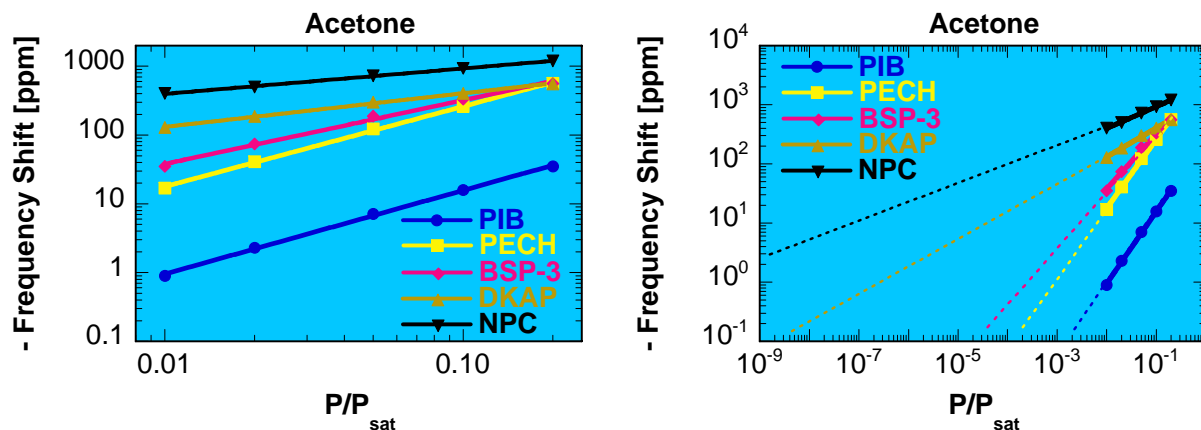


**Figure 4.4:** Adsorption isotherms for acetone into the various SAW-coated devices. The graph on the left shows the strong power-law behavior, and the graph on the right extrapolates these results to infer LODs.

Before discussing the behavior of the other analytes in detail, it is worth looking at isotherm data for a VOC like acetone after the coatings have been exposed to a semi-volatile analyte such as DIMP, which does not fully release from the coatings upon removal from the testing ambient. This is shown in fig. 4.5. Note that the SAW responses for acetone are down

significantly for the coatings that acted as preconcentrators of DIMP, seen in fig. 4.3. On the other hand, PIB and PECH behave nearly identical in terms of detecting acetone as they did prior to the DIMP exposure, shown in fig. 4.4. BSP-3 also behaves similar at the lowest concentration measured,  $P/P_{\text{sat}} = 1\%$ . This is not surprising given its drop-off in preconcentration shown in fig. 4.3. These interpretations are confirmed by the extrapolation of the data, shown in the graph on the right. Both NPC and DKAP have acetone LODs that have dropped to near 100 ppb, while the other three polymers behave nearly the same. The NPC-coated SAW device was annealed to 250 °C in N<sub>2</sub> and retested for acetone detection. The result was a complete recovery to the values shown in fig. 4.4.

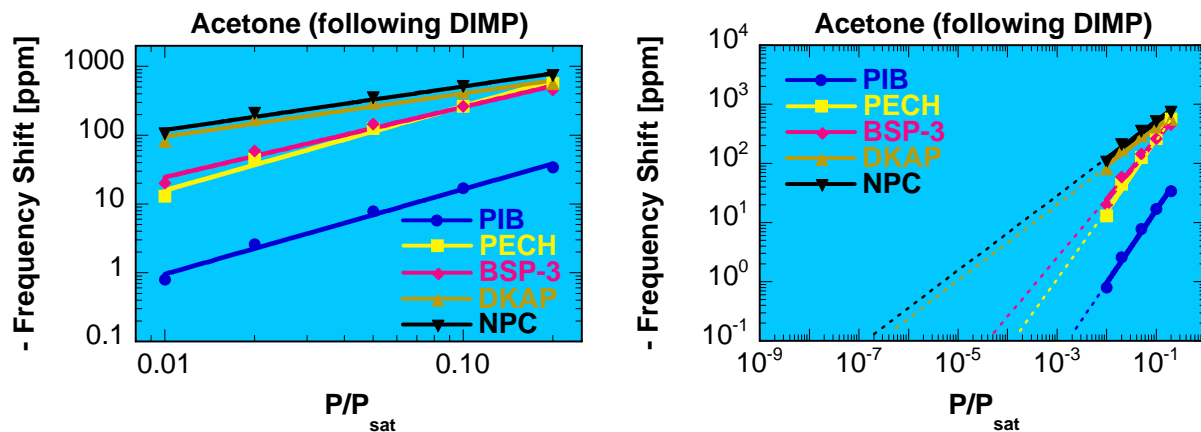


**Figure 4.4:** Adsorption isotherms for acetone following exposure to the semi-volatile DIMP into the various SAW-coated devices. The graph on the left shows the power-law behavior, and the graph on the right extrapolates these results to infer LODs.

The isotherm analysis for the remaining analytes tested all show NPC with superior detection performance as a SAW coating than any of the polymers studied. Fig. 4.5 shows the performance for detection of the aromatic hydrocarbon, toluene. The toluene LOD of NPC is more than eight orders-of-magnitude lower than any of the polymers tested!

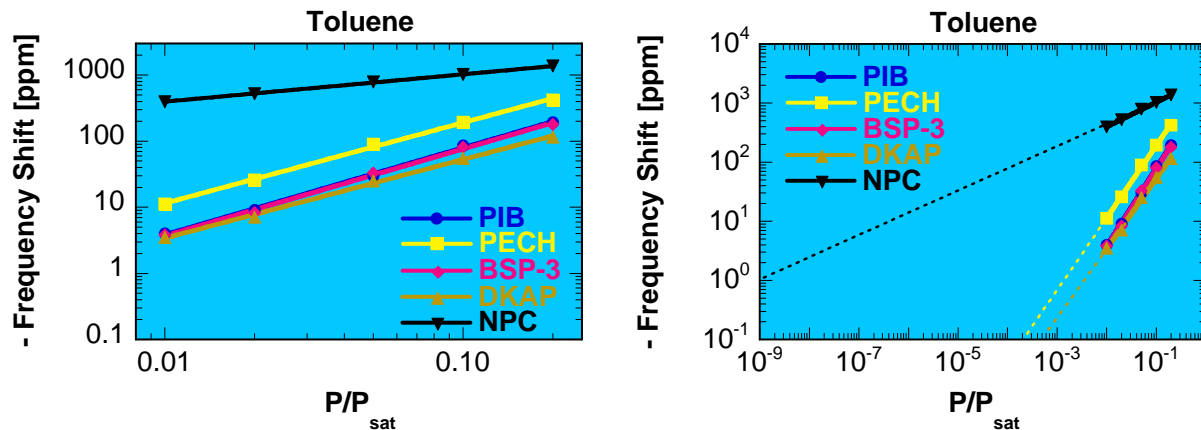


**Figure 4.5:** Adsorption isotherms for toluene into the various SAW-coated devices. The graph on the left shows the power-law behavior, and the graph on the right extrapolates these results to infer LODs.

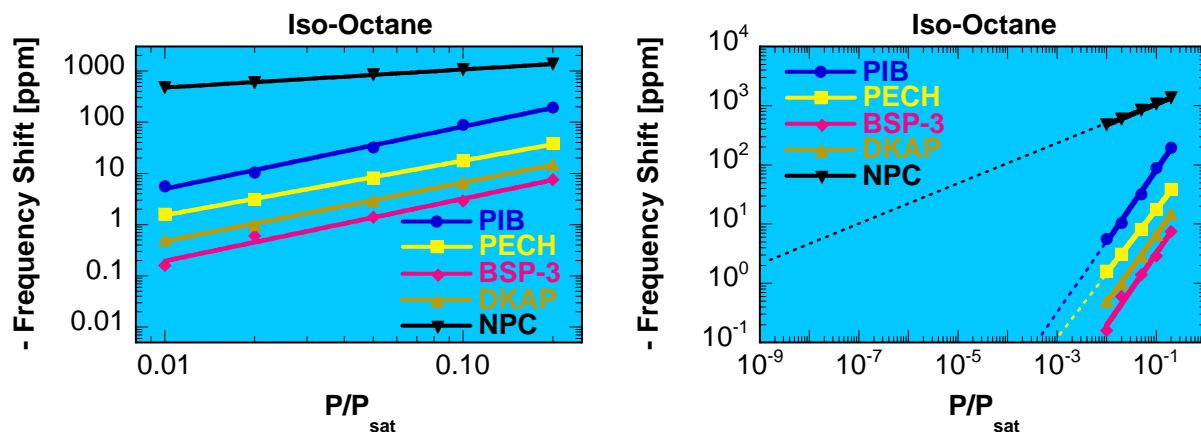


**Figure 4.6:** Adsorption isotherms for iso-octane into the various SAW-coated devices. The graph on the left shows the power-law behavior, and the graph on the right extrapolates these results to infer LODs.

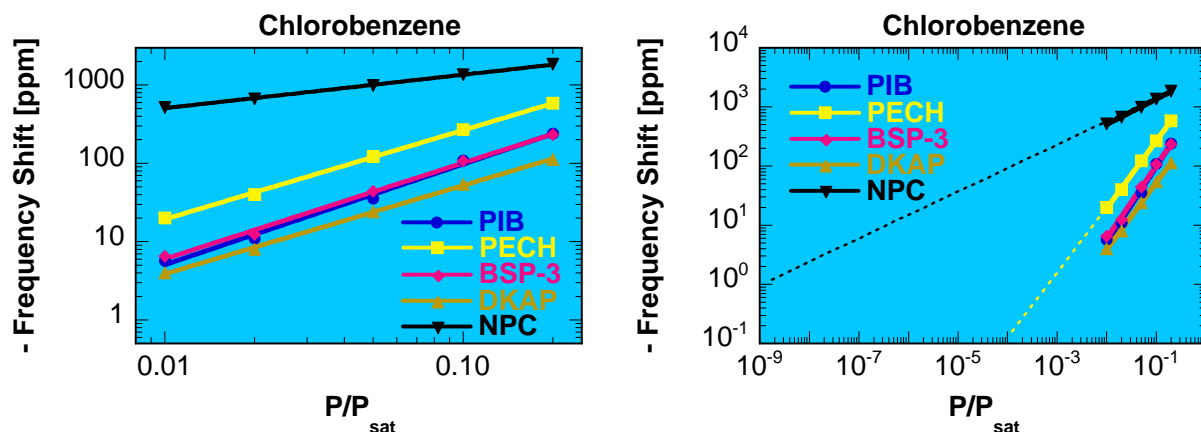


**Figure 4.7:** Adsorption isotherms for chlorobenzene into the various SAW-coated devices. The graph on the left shows the power-law behavior, and the graph on the right extrapolates these results to infer LODs.

Fig. 4.6 and 4.7 show the SAW adsorption isotherms for both iso-octane and chlorobenzene. These two TICs behave somewhat similarly. All of the polymer-coated SAW devices have predicted LODs above 100 ppm, while NPC-coated SAWs have an LOD 7 – 8 orders of magnitude lower. Ppb detection of these two TICs appears to be readily attainable.

Fig. 4.8 shows the SAW adsorption isotherms for trichloroethylene (TCE). TCE appears to be more difficult to detect for all of the adsorbent coatings tested. However, again there is a dramatic difference between the performance of NPC versus the polymer coatings. In general, the polymer coatings all behave similarly for TCE detection, with LODs higher than parts per thousand. NPC appears to have an LOD nearly 4 orders of magnitude lower, inferring easy ppm detection for TCE. So even for this somewhat more difficult analyte to detect, NPC-coated SAWs greatly outperform polymer-coated SAW sensor devices.

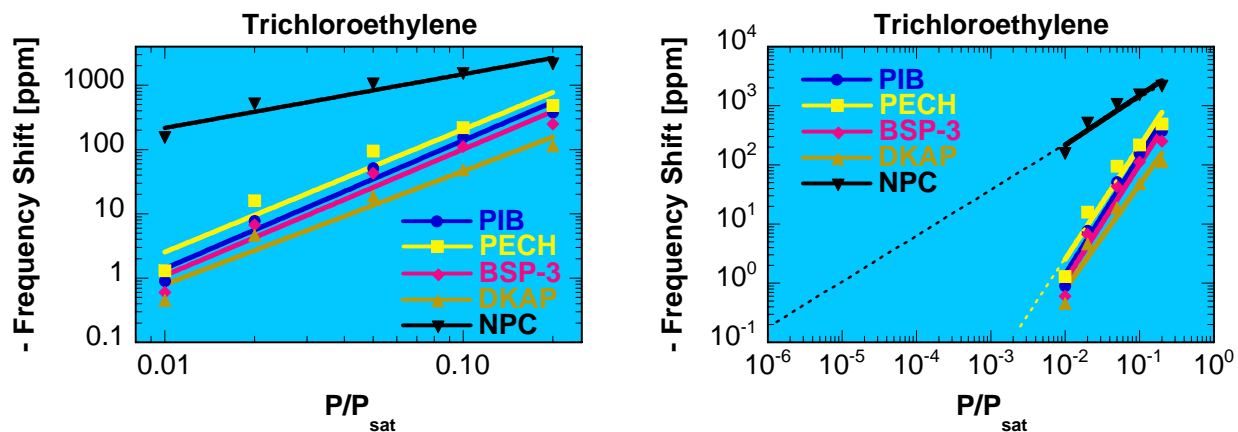


**Figure 4.7:** Adsorption isotherms for trichloroethylene into the various SAW-coated devices. The graph on the left shows the power-law behavior, and the graph on the right extrapolates these results to infer LODs.

One final analyte was studied: a nuclear processing precursor, or NPP. This NPP is required to be used for the fabrication of certain critical components of nuclear weapons. The detection of this NPP is obviously important for National Security and nuclear non-proliferation. NPC outperformed all the polymers as a SAW coating by multiple orders of magnitude, similar to every other analyte studied.

In summary, we show that NPC films grown at room-temperature by pulsed-laser deposition have extremely high-affinity for volatile groups. The adsorption isotherm data using SAW devices suggests possible parts-per-billion detection for many volatile organic compounds and toxic industrial chemicals. Furthermore, results presented here for DIMP, as well as those published earlier for DMMP, show that NPC has good retention properties for semi-volatile chemicals (in this case, nerve gas simulants), indicating the use of NPC as a preconcentrator material. Finally, it must be emphasized that these chemical adsorption experiments using SAW devices clearly show that NPC is not an incremental improvement upon the commonly used polymer materials for gas-phase sensors, rather, NPC represents a revolutionary new material enabling detection of gas analytes in concentrations that are multiple (3 – 8) orders-of-magnitude below that achievable by polymer-coated devices. Note, this is 1,000 to 100,000,000 times greater sensitivity than the current state-of-the-art!

## References:

<sup>1</sup> M. P. Siegal, D. L. Overmyer, R. J. Kottenstette, D. R. Tallant, and W. G. Yelton, Appl. Phys. Lett. **80**, 3940 (2002).



## V. Summary

This project met nearly all of its goals. Nanoporous-carbon (NPC) networks were determined as a function of mass density. NPC structure was optimized for surface acoustic wave (SAW) device microsensor sensitivity. Record-breaking adsorption for various analyte gases, including volatile organic compounds, toxic industrial chemicals, and nuclear processing precursors was measured. A simple model was proposed and validated to predict the adsorption behavior of any coating on a SAW device in low concentrations. Only analyte selectivity via NPC-doping was not accomplished, although, alternate routes were proposed due to the results from this project.

NPC growth by pulsed-laser deposition (PLD) is more complex than first believed. It now appears that serendipity played a role in first discovering NPC and its tremendous potential as a chemical gas adsorbent. Many PLD parameters are critical to the growth of controlled NPC. The laser energy density used to ablate pyrolytic graphite controls the carbon cluster sizes used for NPC film growth. If the clusters are too large, then the resulting film ‘grains’ are not well-connected and cannot support an acoustic wave in SAW devices; we showed that SAW sensor sensitivity is directly related to the film acoustic loss. If the clusters are too small, then they deposit in such a manner that precludes the development of sufficient surface area for analyte adsorption. A laser energy density range exists to ablate ideally-sized carbon clusters. Furthermore, the laser beam must be homogeneous; laser-induced defects into the optics create inhomogeneous beams which lead to mixed structure NPC films with reduced cluster connectivity.

Transmission electron microscopy performed on high-functioning microsensor NPC film material identifies two nano-structural features that help explain the superb chemical adsorption in NPC. First, 1 – 2 nm voids exist throughout the material. While such voids are similar in size to fullerenes, such molecules are not identified in the images; rather, they likely represent the smallest possible structures curved graphene sheet fragments can make to enclose small volumes. Second, and perhaps more importantly, the interplanar spacing between graphene sheet fragments increases with decreasing density. Molecular intercalation into graphite is well-known; expanding the spacing between graphene sheets should improve analyte diffusion in and out of the film.

NPC coatings for SAW devices were compared directly with several commonly used polymer coatings for a wide range of analytes. In all cases, NPC out-performs every polymer coating by multiple orders-of-magnitude in terms of SAW signal response and predicted analyte limits-of-detection (LOD). These results are revolutionary. Furthermore, NPC is stable to higher temperatures than any of the polymers, leading to significantly longer working lifetimes, especially in preconcentrator applications that require the coating to be heated to purge the analyte into another sensor device.



We demonstrated that every SAW coating material obeys a power-law functionality of mass adsorbed versus analyte concentration in the ambient. This new understanding of SAW microsensor device behavior enables extrapolation of device performance to levels well below those measured in the laboratory. Extrapolation of analyte data from every polymer coating tested suggests that such devices will not be able to achieve LODs  $< 10 - 1000$  parts-per-million, depending on the analyte. However, NPC-coated SAW data suggest LODs  $< 1$  part-per-billion for all but one analyte tested, and even for trichloroethylene, NPC-coated SAW LODs are 1000x lower than any polymer-coated SAW tested.

## **VI. Publications and Presentations**

This section lists publications and presentations resulting from this project.

### **Publications**

“Nanoporous-carbon films for gas microsensors,” M. P. Siegal, W. G. Yelton, D. L. Overmyer, and P. P. Provencio, *Langmuir*, **20**, 1194 (2004).

### **Presentations**

“Nanoporous-carbon for chemical microsensors,” *M. P. Siegal*, W. G. Yelton, D. L. Overmyer, and P. P. Provencio, Meeting of the Electrochemical Society, Orlando, FL, October, 2003.

“Nanoporous-carbon: a revolutionary new material for chemical gas microsensors,” W. G. Yelton, *M. P. Siegal*, D. L. Overmyer, and A. W. Staton, Meeting of the Electrochemical Society, San Antonio, TX, May 9 – 14, 2004.

# Distribution List

<b>Copies</b>	<b>Mail Stop</b>	<b>Name</b>	<b>Org.</b>
1	123	LDRD Office, Donna Chavez	1011
3	1421	Michael P. Siegal	1126
1	1421	Donald L. Overmyer	1126
1	1421	Paula Provencio	1111
1	1421	George A. Samara	1130
1	601	Bob Biefeld	1126
1	1056	Barney Doyle	1111
1	1425	Graham Yelton	1743
1	603	Jim Hudgens	1743
1	1425	Al Staton	1764
2	899	Technical Library	9616
1	9018	Central Technical Files	8945-1
1	892	Richard Cernosek	1764
1	892	Joe Simonson	1764
1	603	Ron Manginell	1764
1	1425	Alex Robinson	1764
1	892	Pat Lewis	1764
1	1078	Steve Martin	1707